Advancing Tunnel Boring Machine Performance Prediction in Massive and Highly Fractured Granite: Integrating Innovative Deep Learning and Block Model Techniques

N. Monthanopparat[1] and T. Tanchaisawat[1]
[1]*Department of Civil Engineering, Faculty of Engineering, Chiang Mai University, Chiang Mai 50200, Thailand*
E-mail: nantapol_mon@cmu.ac.th

ABSTRACT: Tunneling projects encounter challenges in predicting Rate of Penetration (ROP), often leading to cost overruns. This study introduces a deep learning approach, combining Deep Feed Forward (DFF) and Long-Short Term Memory (LSTM) techniques to enhance the accuracy of ROP prediction. Focused on the Mae Tang - Mae Ngad Project and its geological complexities in massive and highly fractured granite rock conditions, the research aims to improve ROP predictions. The study demonstrates substantial improvements, revealing Root Mean Square Error (RMSE) values of 0.162 (m/h) for DFF and 0.216 (m/h) for LSTM. Notably, the models exhibit enhanced performance in massive rock conditions with an RMSE of 0.110 (m/h), while highly fractured granite shows an RMSE of 0.261 (m/h). These findings underscore the potential for more precise predictions, addressing historical inaccuracies that often lead to cost overruns ranging between 50 and 900 percent. Integrating deep learning techniques proves valuable, offering a pathway for more reliable and cost-effective tunnel construction endeavors.

KEYWORDS: Tunnel Boring Machine, Deep Learning Technique, Hard Rock Tunneling, and TBM Performance Prediction Model.

1. INTRODUCTION

Tunneling, a pivotal facet of infrastructure development spurred by economic and population growth, faces inherent risks in construction, including geological challenges, construction methods, and management issues, often resulting in cost overruns and delays, such as those observed in the Attiko Metro Project in Greece and Troy and Greenfield Railroad Project in the USA, with cost overruns ranging between 50% and 900%, respectively (Paraskevopoulou and Boutsis, 2020). To mitigate these challenges, predictive models, integrated with estimation techniques like cutter wear and adherence to contract management regulations, have been proposed and applied throughout various project stages, enhancing reliability and overall performance (Bruland, 2000a).

Predicting the Rate of Penetration (ROP) in tunneling involves two main model categories. Theoretical Models, rooted in laboratory testing and full-scale cutting tests, focus on cutting force measurements, aiding machine design, and optimizing thrust-torque tradeoffs. Empirical Models, incorporating field observation data, consider machine performance and rock mass properties, significantly impacting performance parameters (Rostami, 2016). Detailed in Table 1, existing models encompass both theoretical and empirical approaches, incorporating parameters from intact rock to machine specifications. Recent advancements involve machine learning applications, as shown in Table 2, where various algorithms and input parameters contribute to predictive accuracy.

The evolution of these models traces back to their origin as theoretical models in 1976. Tunnellers subsequently developed models with field observation data until computers became suitable for AI technology in recent decades. Figure 1 illustrates that machine learning has played a more dominant role in prediction compared to other types.

Despite the widespread use of prediction models in project planning, their accuracy often falls below expectations (AACE, 2005), resulting in cost overruns and impacting project contingencies. For instance, applying eight existing models to the Mae Tang - Mae Ngad Project (MTMG) yielded root mean square errors (RMSE) between actual and predicted ROP values ranging from 0.356 to 0.893 (Table 3). Accurately predicting tunnel alignment is complicated by challenges in determining crucial rock properties such as the uniaxial compressive strength. This is especially difficult in studies involving massive granite rock and highly fractured granite rock (Pandey et al., 2020).

Table 1 Appearance of existing models in relevant research

Model	Input Parameter														
	Intact Rock Parameter					Rock Mass Properties				Machine & Performance Parameter					
	I1	I2	I3	I4	I5	R1	R2	R3	R4	M1	M2	M3	M4	M5	M6
CSM (Rostami, 1997)	x	x									x	x	x	x	x
MCSM (Yagiz, 2002)	x	x	x			x	x				x	x	x	x	x
Yagiz (Yagiz, 2006)	x	x	x			x	x								
NTNU (Bruland, 2000b)				x	x	x	x				x		x	x	
Mod. NTNU (Macias, 2016)				x	x	x	x				x		x	x	
Gerhing (Gerhing, 1995)	x					x	x				x		x	x	
Alpine (Wilfing, 2016)	x	x				x	x				x		x	x	
Farrokh (Farrokh et al., 2012)	x							x	x	x				x	

Remarks: I1- Uniaxial Compressive Strength, I2- Brazilian Tensile Strength, I3- Density, I4- Drilling Rate Index, I5- Porosity, R1- Distance between planes of weakness, R2-Angle between the plane of weakness and TBM driven direction, R3- Rock Type, R4- Rock Quality Designation, M1- Tunnel Diameter, M2- Cutter Disc Spacing, M3-Cutter Tip width, M4-Cutter disc diameter, M5-Thrust Force and M6- Total Torque.

Table 2 Some reviews on machine learning model in tunneling

Author	Algorithm	Data input	Output	Evaluation
Hadi Fattahi & Nima Babanouri (Fattahi and Babanouri, 2017)	SVR-DE SVR-ABC SVR-GSA	UCS, BI, DPW, Alpha angle	ROP	MSE = 0.0145 MSE = 0.0178 MSE = 0.0158
Danial Jahed Armaghani (Armaghani et al., 2018)	GEP Equation	RQD, UCS, RMR, BTS, WZ, TF, RPM	ROP	RMSE = 0.264
Feng Shangxin (Shangxin et al., 2021)	Deep Learning	Torque, Thrust, RPM, Advance velocity	FPI	RMSE = 2.290
Mohammadreza Koopialipoor (Koopialipoor et al., 2019)	Group method of data handling	RQD, UCS, RMR, BTS, WZ, TF, RPM	ROP	R2 = 0.924
Mohammadreza Koopialipoor (Koopialipoor et al., 2020)	ANN FA-ANN	RQD, UCS, RMR, BTS, WZ, TF, RPM	ROP	R2 = 0.889 R2 = 0.936

Remarks: SVR-Support vector regression, DE-Differential Evolution algorithm, ABC-Artificial Bee Colony algorithm, GSA-Gravity Search Algorithm, GEP-Gene Expression Programming Equation, ANN-Artificial neural network, FA-Firefly algorithm, UCS-Uniaxial Compressive Strength, BI-Brittleness Index, DPW-Distance Between Planes of Weakness, Alpha angle-angle between plane of weakness and TBM direction, RQD-Rock Quality Designation, RMR-Rock Mass Rating, BTS-Brazilian Tensile Strength, WZ-Weathering Zone, TF-Thrust Force, RPM-Cutterhead Velocity, FPI-Field Penetration Index, ROP- Rate of Penetration.

Table 3 Result of existing TBM performance prediction models

Model	Model evaluation		
	All Rock Type RMSE	Rock Type I RMSE	Rock Type II RMSE
CSM (Rostami, 1997)	0.499	0.356	0.743
MCSM (Yagiz, 2002)	0.690	0.764	0.460
Yagiz (Yagiz, 2006)	0.438	0.430	0.457
NTNU (Bruland, 2000)	0.816	0.787	0.885
MNTNU (Macias, 2016)	0.809	0.787	0.861
Gehring (Gerhing, 1995)	0.629	0.481	0.893
Alpine (Wilfing, 2016)	0.514	0.390	0.736
Farrokh (Farrokh, 2012)	0.444	0.422	0.493

Remarks: RMSE - Root mean square errors (m/h),
Rock Type I - Rock without plane of weakness,
Rock Type II - Rock with the plane of weakness.

In response to these challenges, this paper endeavors to develop a predictive model for Tunnel Boring Machine (TBM) performance during the construction phase. Deep learning techniques, specifically Deep Feed Forward (DFF) and Long-Short Term Memory (LSTM), will be employed, integrating with block models based on mining techniques. This innovative approach aims to enhance the accuracy of tunneling performance predictions, contributing to more effective project planning and execution. Additionally, the study will rigorously analyze the output of predictions in massive granite rock and highly fractured granite rock, providing valuable insights into the model's performance under diverse geological conditions.

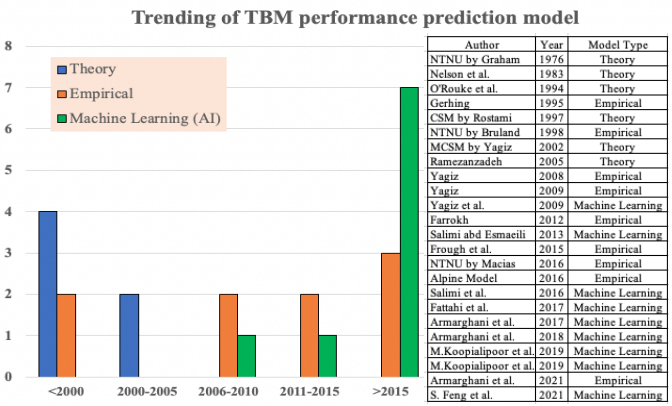

Author	Year	Model Type
NTNU by Graham	1976	Theory
Nelson et al.	1983	Theory
O'Rouke et al.	1994	Theory
Gerhing	1995	Empirical
CSM by Rostami	1997	Theory
NTNU by Bruland	1998	Empirical
MCSM by Yagiz	2002	Theory
Ramezanzadeh	2005	Theory
Yagiz	2008	Empirical
Yagiz	2009	Empirical
Yagiz et al.	2009	Machine Learning
Farrokh	2012	Empirical
Salimi abd Esmaeili	2013	Machine Learning
Frough et al.	2015	Empirical
NTNU by Macias	2016	Empirical
Alpine Model	2016	Empirical
Salimi et al.	2016	Machine Learning
Fattahi et al.	2017	Machine Learning
Armarghani et al.	2017	Machine Learning
Armarghani et al.	2018	Machine Learning
M.Koopialipoor et al.	2019	Machine Learning
M.Koopialipoor et al.	2019	Machine Learning
Armarghani et al.	2021	Empirical
S. Feng et al.	2021	Machine Learning

Figure 1 Trending of TBM prediction model

2. PROJECT DESCRIPTION

2.1 MTMG Water Transfer Tunnel Project – Contract 1

As part of a broader infrastructure initiative, the MTMG project has a primary focus on addressing water supply challenges by transferring water from the Mae Tang River to the Mae Kuang reservoirs. Specifically, the project encompasses a bifurcated tunnel spanning 25 km in its initial segment, dedicated to facilitating water transportation from the Mae Tang River to the Mae Ngad reservoir (refer to Figure 2 and Table 4). Subsequently, the second section of the tunnel is committed to transferring water from the Mae Ngad reservoir to the Mae Kuang reservoir. The overarching goal of the MTMG project is to significantly enhance the water supply for residents residing in Chiang Mai and Lamphun Province, both situated in Northern Thailand. This vital infrastructure endeavor aims to alleviate water scarcity concerns and contribute to the sustainable development of the region.

The tunneling process for the MTMG project is intricately designed and divided into four distinct components, namely, Mae Tang - Mae Ngad contracts 1 and 2, and Mae Ngad - Mae Kuang contracts 1 and 2. Each of these components plays a crucial role in the seamless execution of the project, ensuring the efficient and reliable transfer of water across the specified segments.

By delineating the tunneling process into these well-defined components, the project management aims to enhance precision, streamline construction activities, and optimize resource utilization, ultimately contributing to the successful realization of the project's overarching water supply objectives.

2.2 Geological Conditions along the MTMG Project

A comprehensive geological assessment of the project reveals the presence of three distinct zones. Zone I is characterized by Triassic granitoid and felsic volcanic rock, Zone II encompasses the Ping River fault, and Zone III is defined by sedimentary rock formations (refer to Figure 3). The geological composition of each zone plays a critical role in influencing the tunneling process and determining the challenges associated with the excavation.

Within this geological framework, the Tunnel Boring Machine (TBM) excavation primarily occurs in Zone I. This zone, delineated by granite and marble, presents sporadic instances of high fracture and fault occurrences. This paper specifically focuses on the geological conditions within Zone I, particularly examining the section spanning ring numbers 2350 to 2649, equivalent to 420 meters. This segment is characterized by massive and highly fractured granite, as depicted in Figure 4, with uniaxial compressive strength (UCS) values ranging between 177 and 32 MPa. By delving into the geological nuances of this specific zone, the study aims to provide a detailed understanding of the challenges and considerations pertinent to the tunneling activities within this scope.

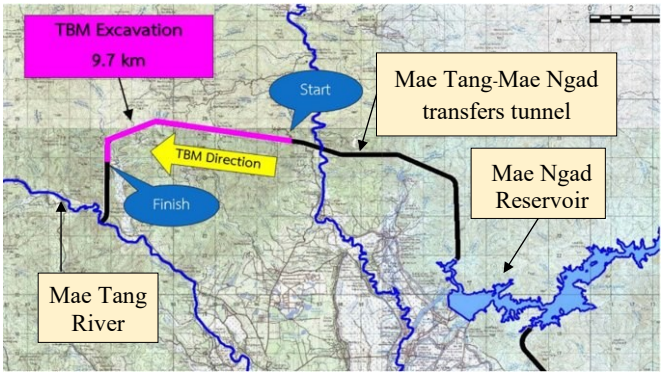

Figure 2 MTMG water transfer tunnel

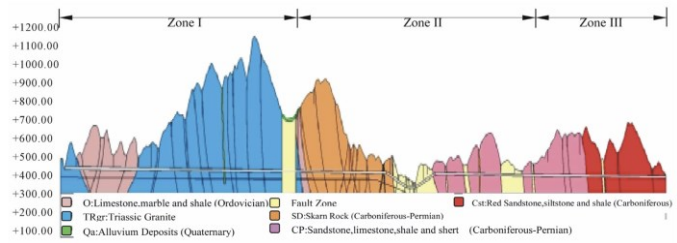

Figure 3 Geological conditions along the MTMG tunnel (Kaewkongkaew et al., 2013)

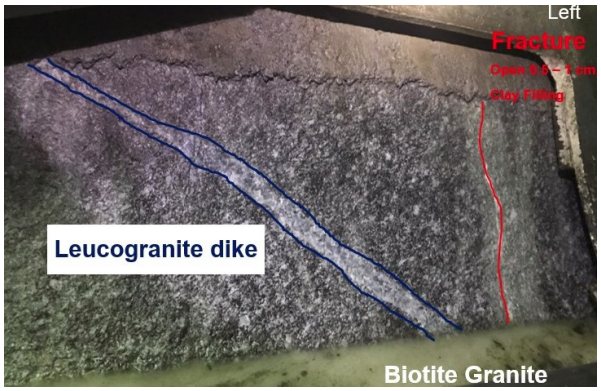

Figure 4 Left side of tail shied opening at ring no. 2484

Table 4 Information of MTMG tunnel project (Mae Tang - Mae Ngad contracts 1)

Description	Value	Remarks
Tunnel length	13.6 km	Main Tunnel
Inner diameter	4.0 m	
Tunneling method	2	
- Drill & Blast	3.9 km	Sta.0+000 to 3+700 and Sta.13+400 to 13+600
- TBM	9.7 km	Sta.13+400 to 3+700
Support system		
- Drill & Blast	Concrete Lining	Horseshoe shape
- TBM	Concrete Segmental	Honeycomb type

2.3 TBM Specification

The tunnel boring machine (TBM) chosen for this project is a hard rock double shield TBM specifically designed to navigate challenging geological conditions. Ascending with a slope of 0.156% from Adit-2 to Adit-1, the TBM ensures efficient excavation throughout the tunneling process. With an excavation diameter of 4.74 meters, the TBM is equipped with 32 cutter discs, each measuring 17 inches (432 mm) in diameter. The cutter discs are arranged with an average spacing of 82 mm, contributing to precision in the excavation process.

The TBM boasts a maximum thrust of 7,500 kN, allowing it to navigate through diverse geological formations encountered during the project. Operating at a cutterhead speed ranging from 0.5 to 0.9 revolutions per minute (rpm), the machine adapts to different rock conditions. Powering these operations are six drive motors, collectively enabling the TBM to execute precise and efficient excavation. As an integral part of the backup system, rolling stock is incorporated for material supply and muck hauling, ensuring a streamlined process for handling excavated material and supplying resources required for tunneling activities (Figure 5). These technical specifications collectively highlight the TBM's suitability for the specified geological conditions and the demands of the project.

Figure 5 Illustrate T57 double shield TBM and rolling stock fleets

3. DEEP LEARNING TECHNIQUE

Deep learning, a branch of machine learning, has been extensively adopted for its ability to efficiently process complex data structures through artificial neural networks (ANNs) with multiple layers.

In geotechnical engineering, particularly in tunneling, the integration of machine learning techniques has proven transformative. For instance, Hadi Fattahi and Nima Babanouri utilized SVR variants enhanced with different optimization algorithms to predict the Rate of Penetration (ROP) with low mean squared errors, demonstrating high accuracy in predictions (Fattahi and Babanouri, 2017). Similarly, Armaghani et al. (2018) applied the Gene Expression Programming (GEP) approach, using factors like Rock Quality Designation (RQD) and Uniaxial Compressive Strength (UCS) to predict ROP with an RMSE of 0.264. Furthermore, Feng Shangxin et al. (2021) explored the use of deep learning for predicting the Field Penetration Index (FPI) with data inputs like torque and thrust, highlighting the technique's robustness despite a higher RMSE of 2.290. Moreover, Koopialipoor et al. demonstrated the effectiveness of the Group Method of Data Handling (Koopialipoor et al., 2019) and Artificial Neural Networks (Koopialipoor et al., 2020) in predicting ROP with high R^2 values, underlining the predictive power of these approaches.

Building upon this empirical foundation, this paper explores the use of two distinct deep learning structures tailored to different types of data encountered in tunneling operations. The Deep Feed Forward (DFF) network will be employed to handle non-sequential data, such as the physical properties of rock masses, which do not require consideration of previous states or time dependencies. This makes DFF particularly suited for analyzing static inputs like mineral composition and grain size distribution. On the other hand, the Long Short-Term Memory (LSTM) network will be utilized specifically for sequential or time series data, such as monitoring data collected over the course of tunneling. This approach takes advantage of LSTM's capacity to remember and utilize past information, which is crucial for accurately predicting the temporal sequence of events, like rock deformation or tool wear. By applying these models independently, we aim to maximize the predictive accuracy of tunnel boring machine performance in the challenging geological conditions of massive and highly fractured granite.

3.1 Deep Feed Forward Network (DFF)

A fundamental architecture in the realm of deep learning, the deep feed-forward network (DFF) is distinguished by its multilayer structure, comprising an input layer, several hidden layers, and an output layer (refer to Figure 6). This architecture facilitates a unidirectional flow of information from the input to the output layer, allowing each node within a hidden layer to connect to every node in the preceding layer. Such a setup enables the network to construct intricate hierarchical representations of the input data, which is essential for analyzing non-sequential data relevant to tunneling projects, such as rock mass properties and geological conditions.

DFFs are particularly adept at handling large, static datasets where temporal relationships are not a concern, making them ideal for predicting aspects like tool wear or estimating the penetration rate of TBMs based on geological parameters. The effectiveness of DFFs in tunneling stems from their ability to autonomously identify and learn from the complex, hierarchical features of geological data, thereby enhancing predictive accuracy and operational efficiency in tunnel construction.

3.2 Long Short-Term Memory Network (LSTM)

Within the spectrum of deep learning architectures, the Long Short-Term Memory network (LSTM) specifically addresses the limitations of traditional recurrent neural networks (RNNs), as depicted in Figure 7. Originating in 1997 from the pioneering work of Sepp Hochreiter and Juergen Schmidhuber, LSTMs enhance the basic RNN structure by incorporating memory cells and various gates that manage the flow of information (Hochreiter and Schmidhuber, 1997). This design effectively overcomes the notorious gradient vanishing problem associated with extended data sequences. The advanced structure of LSTMs is detailed in Figure 8, highlighting the unique components such as input gates, forget gates, and output gates.

The LSTM's ability to maintain and utilize long-term data sequences is particularly valuable in tunneling applications where sequential or time-series data, such as the continuous monitoring of TBM operational parameters, is crucial. LSTMs excel in modeling the dynamics of tunnel advancement, adapting to changes in geological conditions over time, and predicting potential issues before they arise. By capturing and analyzing patterns over extended periods, LSTMs facilitate more accurate forecasts of machine behavior and project timelines, thereby contributing to safer and more cost-effective tunneling operations.

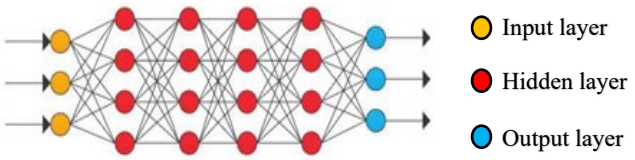

Figure 6 Deep feed forward network (DFF)

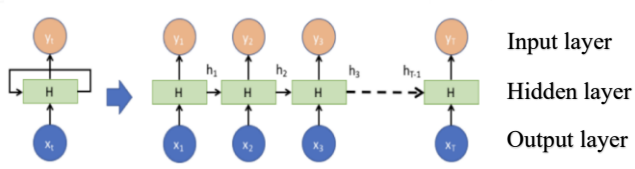

Figure 7 Recurrent neural network (RNN)

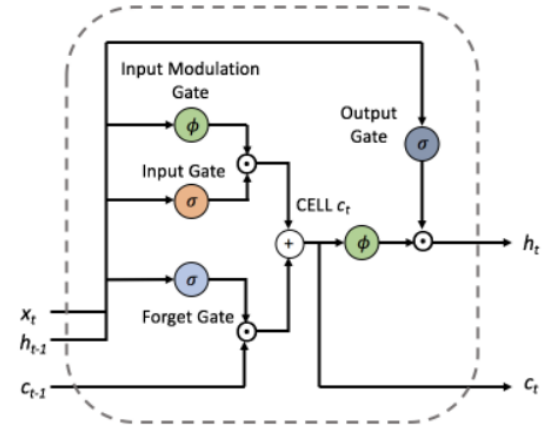

Figure 8 Illustrates the structure of long short-term memory (LSTM) (Sirinart, 2017).

4. BLOCK MODEL TECHNIQUE

In tunneling, acquiring comprehensive data on intact rock properties, such as unconfined compressive strength (UCS), is often challenging due to the practical limitations of examining the entire length of a tunnel. Techniques like the use of a Schmidt hammer provide indirect measurements of UCS along the penetrated path. Initially developed for concrete testing in 1948, the Schmidt hammer has been adapted to assess the compressive strength of rock both in-situ and in the laboratory. The tool measures the rebound value of a hammer after it impacts the rock surface, which correlates to the rock's compressive strength.

From various studies, it has been found that the Schmidt hammer is particularly effective in geotechnical evaluations. For instance, Ghaemi et al. utilized this tool to measure the compressive strength of rock mass in the project of Emamzadeh Hashem Tunnel, Amol, Iran (Ghaemi et al., 2015). Their findings showed that the correlation between the UCS and the indirect method had a Root Mean Square error ranging between 14.73 and 20 percent, with R^2 values from 0.723 to 0.840, highlighting its utility in practical applications.

However, in the context of double shield-type Tunnel Boring Machines (TBMs), the presence of shields complicates direct rock investigations, often leading to gaps in UCS data. This specific challenge is visually depicted in Figure 9, illustrating how shield presence can obstruct rock property assessment along the tunnel route.

To address these challenges, this research proposes the adoption of a mining technique known as the “Block Model.” Traditionally used in mining to evaluate ore properties such as lithology, grade percentage, density, and hardness, the Block Model is adapted here for geological evaluation in tunneling. The method involves dividing the geological data into discrete “blocks” or “bricks,” where the size of each block is determined by its geological characteristics and the required precision for assessment. This structured approach allows for a detailed, localized analysis of rock properties along the tunnel route, as depicted in Figure 10 (Poniewierski, 2019).

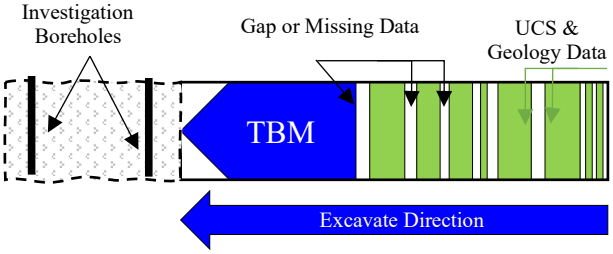

Figure 9 Display gaps UCS and Geological data

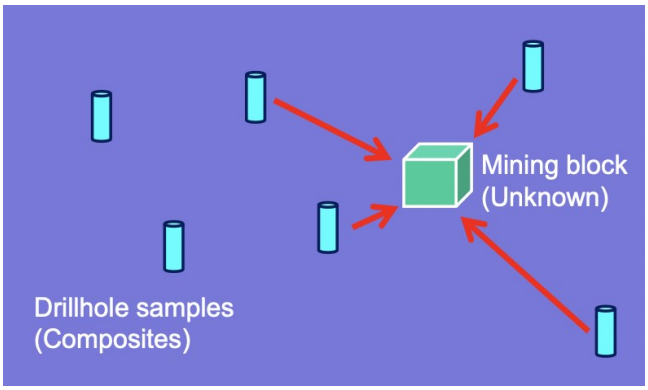

Figure 10 Display of the estimation of drillhole samples into a block

The Block Model facilitates the simultaneous assessment of multiple rock properties within these blocks using the available data, significantly enhancing the understanding of geological variations along the tunnel. For areas within the tunnel where data varies minimally over significant distances, the Inverse Distance Weighting (IDW) Method proves particularly effective. This spatial interpolation technique estimates the properties of unknown points based on the properties of nearby known points, with closer data points receiving greater weighting. The general formula for the IDW employed in this study is given by:

$$G_A = \sum_{i=1}^{n} W_i G_i \quad (1)$$

Where, G_A = estimated grade; W_i = normalizes weight; G_i = Grade. The summary of W_i equals to 1. W_i can be calculated using the equation as:

$$W_i = 1/d_i^x \quad (2)$$

Where, x = initial value that is equals to 2, after that it is adaptive on field.

This enhanced explanation of the Block Model, including the use of the Schmidt hammer for indirect UCS measurements, should clarify its application and utility in tunneling projects, facilitating a better understanding of geological conditions along the tunnel path and enabling more accurate planning and execution.

5. METHODOLOGY

This section outlines the methodology employed in the study, including data collection, data preparation and evaluation processes. Each step is detailed below to ensure a clear understanding of the research approach.

5.1 Data Collection for Model Formation

5.1.1 Geological Data

Geological parameters are gathered from investigated boreholes and surveys along the tunnel line. This data includes the Uniaxial Compressive Strength (UCS), indirect UCS measurements obtained using a Schmidt hammer, Alpha angle, Coarseness Index (CI), and Rock Mass Type (RMT).

5.1.2 TBM Performance Data

Performance data from the tunnel boring machine is continuously recorded via a work tracking program. This includes the duration required for the installation of concrete segments, each segment referred to as a "Ring," covering a tunnel length of 1.4 meters.

5.2 Geological Parameter Extent Using Block Model

The Block Model is instrumental in addressing gaps in geological data, particularly in the measurement of Uniaxial Compressive Strength (UCS). In areas where direct UCS and indirect UCS data are missing, the Block Model helps interpolate these values using the Inverse Distance Weighting (IDW) method, outlined in Equations 1 and 2.

5.2.1 Process of Imputing Missing UCS Values

Initial Data Plotting: Initially, UCS values obtained from borehole data and surveys are plotted on a graph as blue dots (Figure 11). These represent actual measured values along different points of the tunnel.

Second, Imputation Using Block Model: To fill in the gaps where UCS data are missing, the Block Model employs the IDW method. This technique estimates the UCS values based on the spatial proximity and the known UCS values from neighboring points. The imputed UCS values are plotted as yellow dots on the graph (Figure 11). These yellow dots effectively bridge the gaps between the blue dots, providing a continuous understanding of UCS variations along the tunnel.

Resulting UCS Dataset: The final graph, which can be viewed in Figure 11, displays both the original and imputed UCS values. This visual representation helps illustrate how the Block Model facilitates a comprehensive dataset, enhancing geological assessments and subsequent tunneling decisions.

By integrating the actual and imputed data, the Block Model not only fills in missing data but also enhances the reliability of geological evaluations across the tunnel. This comprehensive dataset is crucial for optimizing tunnel design and anticipating challenges that might arise due to varying rock strength.

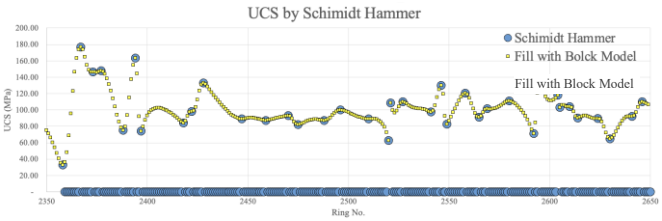

Figure 11 Display of UCS (by Schmidt hammer) and imputed UCS values

5.3 Parameter Selection for Inputs

The input parameters for the predictive model were carefully selected based on data collected from 300 Rings, specifically from Ring Numbers 2350 to 2649. These inputs include a range of operational and geological variables thought to influence the Rate of Penetration (ROP), which is critical for assessing the performance of Tunnel Boring Machines (TBMs). The parameters considered were Thrust Force, Cutterhead Torque, Cutterhead Speed, Rock Mass Type (RMT), and Uniaxial Compressive Strength (UCS).

To determine the most impactful parameters on ROP, a heatmap was created to visually represent the correlation coefficients between each input parameter and ROP. Figure 12 provides this heatmap, which aids in understanding the strength and direction of each relationship:

Thrust Force: This shows a moderate negative correlation with ROP (-0.5), indicating that higher thrust force tends to decrease ROP, possibly due to increased mechanical resistance.

Cutterhead Torque: Exhibits a moderate positive correlation (0.37), suggesting that higher torque may enhance cutting efficiency and thus increase ROP.

Cutterhead Speed: Displays a correlation coefficient of 0.23, indicating a positive relationship with ROP, though less pronounced compared to torque or thrust force.

Rock Mass Type (RMT): Has a moderate positive correlation (0.42), implying that certain rock types may facilitate faster drilling.

Uniaxial Compressive Strength (UCS): This shows a correlation of -0.24, indicating that softer rocks, which have lower UCS values, may allow for higher ROP.

The correlation analysis was instrumental in refining the selection of input parameters for the predictive model. By choosing parameters with statistically significant correlations to ROP, the model is better positioned to accurately predict tunneling performance. The selected parameters reflect a balance between operational variables (thrust force, cutterhead torque, and speed) and geological conditions (rock mass type and UCS), ensuring comprehensive coverage of factors that influence TBM effectiveness. This strategic selection process enhances the model's reliability and ensures it is robust enough for practical application in tunneling operations, aiding in the planning and optimization phases of tunnel construction projects.

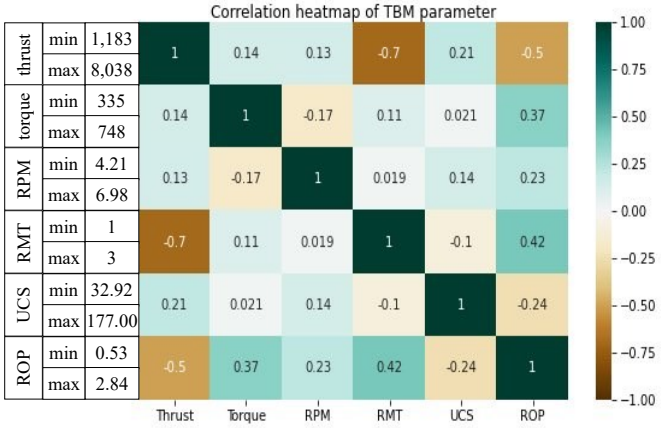

Remarks: units of inputs and output parameters are followings.
Thrust force: kN, Cutterhead torque: kN-m,
Cutterhead Torque (RPM): Round per minute
Rock mass type: No units, UCS: MPa and ROP: m/h

Figure 12 Display of correlation heatmap between the input parameter and the output (ROP)

5.4 Data Preparation before Deep Learning

Effective data preparation is crucial for the optimal performance of deep learning models. This study utilizes two types of neural networks: Deep Feed Forward Network (DFF) and Long Short-Term Memory (LSTM), each requiring specific scaling techniques to prepare the data.

5.4.1 Data Scaling for DFF and LSTM

Before training, data for the DFF model is scaled using Standard Scaling, which transforms the data to have zero mean and unit variance. This normalization method is ideal for DFF models because it prevents features with larger numerical ranges from dominating the learning process, ensuring that each feature contributes equally to the model's predictions. This is particularly beneficial when input features vary in their units of measurement, aiding in faster and more stable convergence during training.

For the LSTM model, data is scaled using Min-Max Scaling to ensure that all features contribute equally to the model's learning process and maintain effective internal state calculations over time. This scaling method transforms the data to a common scale of 0 to 1, aligning with the activation functions used within LSTMs, which are sensitive to the magnitude of input values. This helps stabilize the model's learning and internal dynamics, which is especially important for processing sequential data where maintaining temporal dependencies is crucial.

5.4.2 Data Arrangements

For the DFF model, the order of data is not critical as the model does not process temporal sequences. However, for the LSTM model, it is imperative to arrange the data sequentially. For example, to predict performance at Ring 3000, data from Rings 2990 to 2999 must be organized in sequence after Min-Max Scaling, ensuring the LSTM model accurately captures temporal dependencies.

5.5 Dataset Splitting

The dataset is divided into two parts: 80% for training the machine learning model and 20% for validation. This equates to 240 Rings for training and 60 Rings for validation.

5.6 Performance Evaluation Metrics

The model's performance is assessed using the expected accuracy range specified by AACE (-10% to +15%). Additionally, the Root Mean Square Error (RMSE) is calculated with the following Equation:

$$RMSE = \sqrt{\sum_{i=1}^{N}(\hat{y}_i - y_i)^2/N} \quad (3)$$

Where, $\hat{y}_i$ = predicted ROP values; y_i= achieve ROP value; N= the total numbers of data.

This comprehensive methodology ensures that each step, from data collection through performance evaluation, is meticulously designed to support the study's objectives, enabling effective predictions of TBM performance based on deep learning models.

6. MODEL VALIDATION

The structural configurations for the Deep Feed Forward (DFF) and Long Short-Term Memory (LSTM) models used in the Mae Tang - Mae Ngad Project (MTMG) were meticulously determined through a comprehensive hyperparameter tuning process. For the DFF model, the optimal setup finalized from Table 5 involved configuring the model with 5 hidden layers, each containing 7 nodes. This configuration was chosen after extensive testing to best capture the complexities of the input data relevant to tunneling performance, achieving a minimized RMSE and optimal performance during validation phases. Similarly, the LSTM model, specifically designed to process temporal sequences effectively, was optimized with 10 input nodes and a single hidden layer containing 12 nodes as shown in Table 6. The selection of these configurations was driven by their superior ability to accurately predict the Rate of Penetration (ROP), reflecting the lowest RMSE values and highest validation ratings in comparative testing. These configurations are documented in Tables 5 and 6, illustrating the step-by-step hyperparameter adjustments and their impact on model performance, ensuring that each model is finely tuned to the specific requirements of the MTMG project.

The validation of the prediction models was rigorously conducted using a dataset comprised of over 300 data points spanning Ring numbers 2350 to 2649. The DFF model, depicted in Figure 13, and the LSTM model, shown in Figure 14, underwent evaluation to assess their predictive accuracy. The validation process involved calculating the Root Mean Square Error (RMSE) for both models, with results presented in Figure 15 and summarized in Table 7. Furthermore, the effectiveness of these models in different geological contexts was analyzed and is depicted in Figure 16 and detailed in Table 8, highlighting the models' performance across varying rock mass types.

The comparative analysis between the DFF and LSTM models, alongside established models such as the CSM and Yagiz models, provides a comprehensive perspective on the effectiveness of deep learning techniques in tunneling operations. It is important to note that the comparisons made with the CSM model (Rostami, 1997) and the Yagiz model (Yagiz, 2006) are based on different datasets. These historical models were applied to other geological and operational conditions, which may influence the RMSE values reported. Despite LSTM's capability to utilize sequential data, its RMSE of 0.216 did not significantly outperform the DFF's RMSE of 0.162. Compared to traditional models, both deep learning approaches demonstrated superior accuracy. For instance, the CSM model, which is theoretical, reported an RMSE of 0.499 for all rock mass types, with specific values of 0.356 for Type I (Massive) and 0.743 for Type II (Highly

fractured). Similarly, the empirical Yagiz model yielded RMSEs of 0.438, 0.430, and 0.457 for all rock mass types, Type I and Type II, respectively, as detailed in Table 3.

Table 5 The result of hyperparameter tunning process for DFF structures

Stage & Model No.	No. of hidden layer	No. of node in hidden layer	Learning rate	RMSE (m/h) Training	RMSE (m/h) Validate	Rating Training	Rating Validate	Sum. rating	Rank
Stage 1. Select No. of hidden layer									
1-1	2	5	0.001	0.122	0.189	1	4	5	4
1-2	3	5	0.001	0.109	0.175	2	5	7	1
1-3	4	5	0.001	0.105	0.202	3	2	5	4
1-4	5	5	0.001	0.102	0.194	4	3	7	1
1-5	6	5	0.001	0.094	0.221	5	1	6	3
Results_Stage 1: Select No. of hidden layer = 3 and 5									
Model No. 1-2, Number of hidden layer = 3									
Model No. 1-4, Number of hidden layer = 5									
Stage 2. Select No. of node in hidden layer									
2-1	3	3	0.001	0.144	0.258	2	5	7	13
2-2	3	4	0.001	0.150	0.275	1	3	4	14
2-3	3	5	0.001	0.102	0.198	5	12	17	7
2-4	3	6	0.001	0.101	0.228	6	8	14	11
2-5	3	7	0.001	0.083	0.200	9	11	20	4
2-6	3	8	0.001	0.074	0.174	11	14	25	1
2-7	3	9	0.001	0.074	0.204	11	10	21	3
2-8	3	10	0.001	0.053	0.238	14	6	20	4
2-9	5	3	0.001	0.131	0.314	3	1	4	14
2-10	5	4	0.001	0.120	0.236	4	7	11	12
2-11	5	5	0.001	0.092	0.196	7	13	20	4
2-12	5	6	0.001	0.085	0.219	8	9	17	7
2-13	5	7	0.001	0.081	0.172	10	15	25	1
2-14	5	8	0.001	0.071	0.261	13	4	17	7
2-15	5	9	0.001	0.047	0.302	15	2	17	7
Results_Stage 2:									
Model No. 2-6, No. of hidden layer = 3 and No. of node in hodden layer = 8									
Model No. 2-13, No. of hidden layer = 5 and No. of node in hidden layer = 7									
Stage 3. Select Learning rate									
3-1	3	8	0.0001	0.120	0.184	1	9	10	6
3-2	3	8	0.0005	0.085	0.270	4	1	5	10
3-3	3	8	0.001	0.086	0.188	3	7	10	6
3-4	3	8	0.005	0.066	0.195	8	6	14	2
3-5	3	8	0.01	0.065	0.203	9	5	14	2
3-6	5	7	0.0001	0.109	0.153	2	10	12	4
3-7	5	7	0.0005	0.083	0.211	5	4	9	8
3-8	5	7	0.001	0.070	0.187	7	8	15	1
3-9	5	7	0.005	0.076	0.231	6	3	9	8
3-10	5	7	0.01	0.064	0.267	10	2	12	4
Result_Stage 3:									
Model No. 3-8, No. of hidden layer = 5, No. of node in hodden layer = 7 and learning rate = 0.001									
Remarks: The best of each stage (Training & Validate) were obtained highest score.									

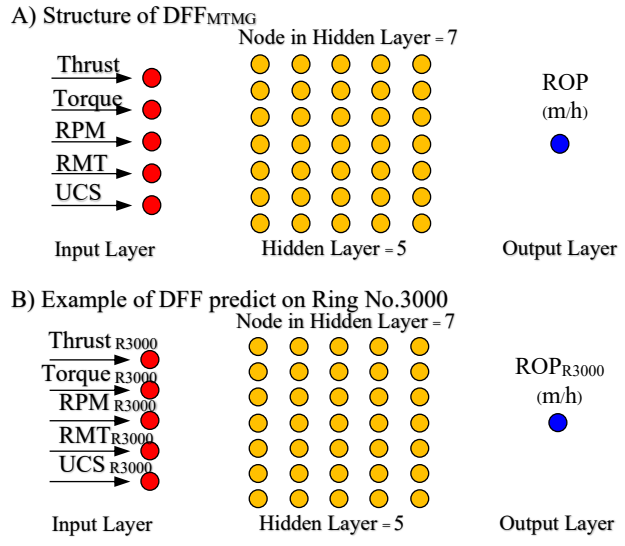

Figure 13 A) Structure of DFF for MTMG prediction model and B) An example for predicted Ring No. 3000

Table 6 The result of the hyperparameter tuning process for LSTM structures

Stage & Model No.	No. of input node	No. of node in hidden layer	Learning rate	RMSE (m/h) Training	RMSE (m/h) Validate	Rating Training	Rating Validate	Sum. rating	Rank
Stage 1. Select No. of input node									
1-1	3	5	0.001	0.147	0.120	1	4	5	10
1-2	4	5	0.001	0.136	0.114	2	9	11	4
1-3	5	5	0.001	0.131	0.113	4	10	14	2
1-4	6	5	0.001	0.127	0.119	5	6	11	4
1-5	7	5	0.001	0.134	0.119	3	6	9	7
1-6	8	5	0.001	0.122	0.129	8	1	9	7
1-7	9	5	0.001	0.127	0.120	5	4	9	7
1-8	10	5	0.001	0.119	0.116	9	8	17	1
1-9	12	5	0.001	0.124	0.124	7	3	10	6
1-10	15	5	0.001	0.109	0.127	10	2	12	3
Results_Stage 1: Select No. of input node = 10									
Stage 2. Select No. of node in hidden layer									
2-1	10	3	0.001	0.122	0.123	4	5	9	8
2-2	10	4	0.001	0.123	0.128	3	1	4	12
2-3	10	5	0.001	0.125	0.120	2	6	8	9
2-4	10	6	0.001	0.119	0.124	6	4	10	7
2-5	10	7	0.001	0.116	0.128	7	1	8	9
2-6	10	8	0.001	0.127	0.120	1	6	7	11
2-7	10	9	0.001	0.113	0.125	8	3	11	6
2-8	10	10	0.001	0.121	0.117	5	10	15	5
2-9	10	11	0.001	0.113	0.117	8	10	18	3
2-10	10	12	0.001	0.108	0.116	11	12	23	1
2-11	10	13	0.001	0.110	0.119	10	8	18	3
2-12	10	15	0.001	0.106	0.119	12	8	20	2
Results_Stage 2:									
Model No. 2-6, No. of hidden layer = 3 and No. of node in hodden layer = 8									
Model No. 2-13, No. of hidden layer = 5 and No. of node in hidden layer = 7									
Stage 3. Select Learning rate									
3-1	10	12	0.0001	0.154	0.138	1	1	2	5
3-2	10	12	0.0005	0.129	0.118	2	4	6	4
3-3	10	12	0.001	0.108	0.117	3	5	8	1
3-4	10	12	0.005	0.079	0.126	4	3	7	2
3-5	10	12	0.01	0.078	0.128	5	2	7	2
Result_Stage 3:									
Model No. 3-8, No. of hidden layer = 5, No. of node in hodden layer = 7 and learning rate = 0.001									
Remarks: The best of each stage (Training & Validate) were obtained highest score;									
These RMSE values are scaling with Min-Max method.									

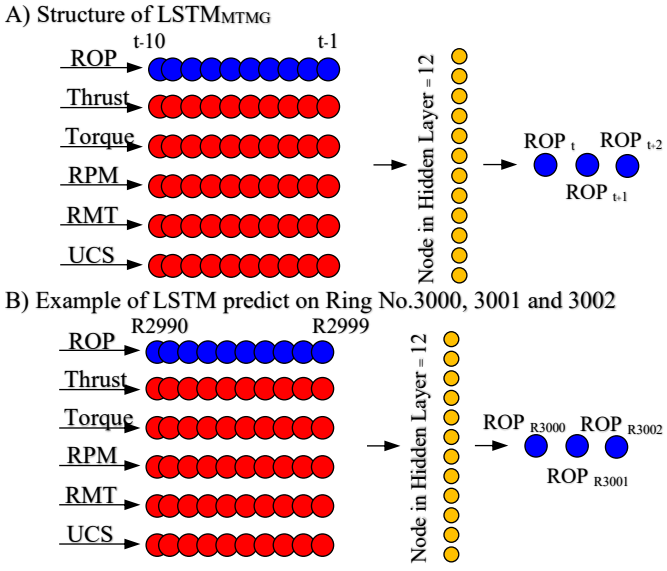

Figure 14 A)Structure of LSTM for MTMG prediction model and B) An example for predicted Ring No. 3000, 3001, and 3002

The results underscore that both DFF and LSTM models provide more precise predictions than these existing models, especially when handling varied geological conditions. DFF stands out for its ability to provide highly accurate predictions, leveraging its structured architecture and layered approach. On the other hand, LSTM demonstrates remarkable adaptability, particularly in scenarios characterized by fluctuating geological conditions and unforeseen

input parameters. Its recurrent neural network design allows it to effectively predict based on historical datasets, making it especially suited for handling dynamic and evolving environments. The combined outputs from both DFF and LSTM models, as presented in Table 8, reveal distinct RMSE values for different rock types, with 0.110 for Massive (Type I) and 0.261 for highly fractured granite (Type II). These results demonstrate the nuanced capability of deep learning models to adapt to and accurately predict performance across different geological scenarios. The detailed analysis in Table 8 was crucial in evaluating the relative effectiveness of these deep learning techniques against varied rock masses, highlighting that deep learning not only offers improvements in predictive accuracy but also provides insights into the specific conditions under which each model excels. This comparative analysis is instrumental for guiding future applications and adjustments of the models, ensuring optimized performance in diverse tunneling environments.

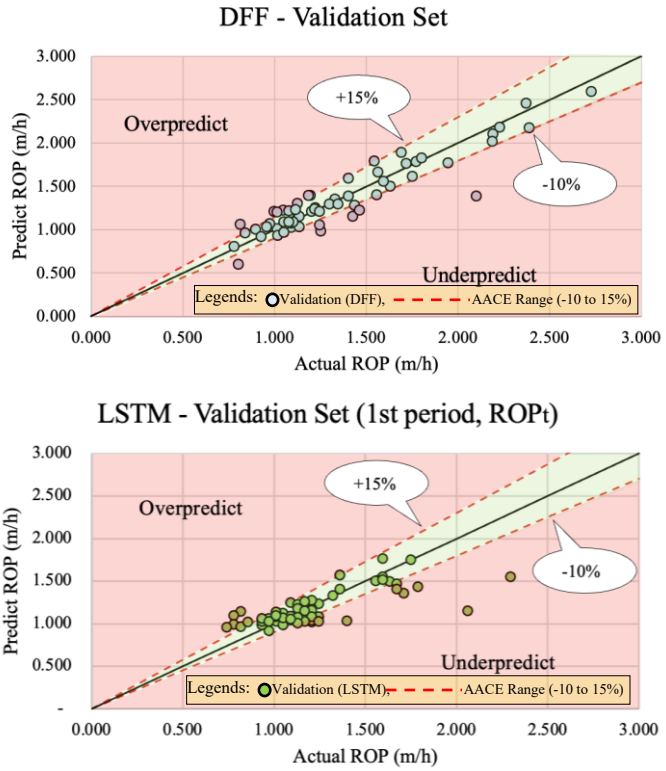

Remarks: Overpredict – Predict ROP higher than Actual ROP
Underpredict – Predict ROP lower than Actual ROP

Figure 15 Predicted ROP value by DFF and LSTM network

Table 7 Output of Prediction Models on Validation Set

Model	Number of datasets	Model evaluation			
		RMSE (m/h)	AACE Range (-10% to +15%)		
			In range	Over perform	Under perform
DFF	60	0.162	44 (73%)	9 (15%)	7 (12%)
LSTM (t)	58	0.216	36 (62%)	8 (14%)	14 (24%)

Remarks: The LSTM model is designed to predict the next three periods based on sequential data. Consequently, the validation dataset for the LSTM model includes only 58 of the 60 datasets allocated. This adjustment is necessary because the last two datasets of the sequence lack sufficient subsequent data points to complete the required three-period prediction cycle. This ensures the integrity and accuracy of the LSTM's predictive performance.

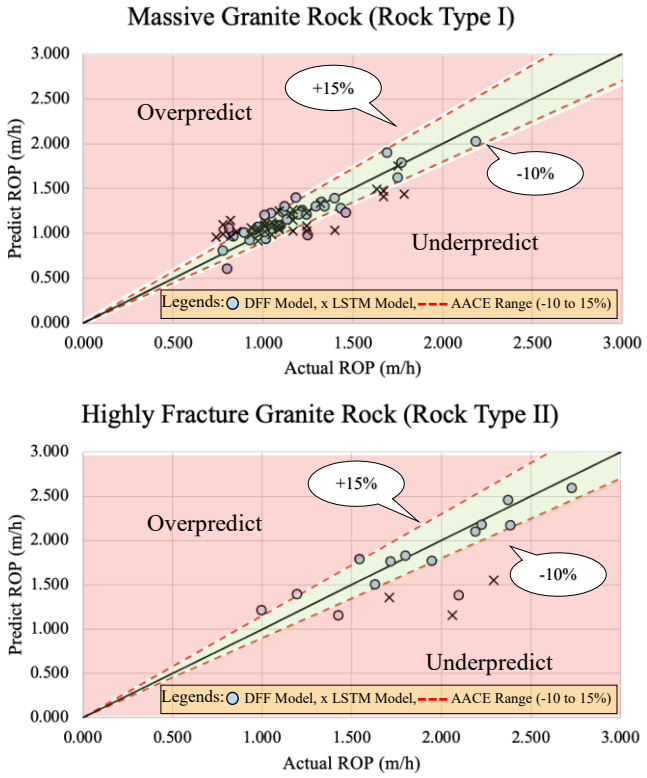

Remarks: Overpredict – Predict ROP higher than Actual ROP
Underpredict – Predict ROP lower than Actual ROP

Figure 16 Predicted ROP on massive and highly fractured granite

Table 8 Output of prediction model on massive and highly fracture granite rock

Rock Mass Type	Number of datasets	Model evaluation			
		RMSE (m/h)	AACE Range (-10% to +15%)		
			In range	Over perform.	Under perform.
Type I					
- DFF	35	0.094	25 (71%)	6 (17%)	4 (12%)
- LSTM	36	0.125	23 (64%)	6 (17%)	7 (19%)
Sum.	71	0.110	48 (68%)	12 (17%)	11 (15%)
Type II					
- DFF	15	0.179	10 (67%)	3 (20%)	2 (13%)
- LSTM	3	0.669	- (0%)	- (0%)	3 (100%)
Sum.	18	0.261	10 (56%)	3 (17%)	5 (28%)

Remarks: Rock Type I – Massive Granite Rock,
Rock Type II – Highly Fracture Granite Rock.

7. CONCLUSIONS

The comprehensive evaluation of the Deep Feed Forward (DFF) and Long Short-Term Memory (LSTM) models within this study illustrates their distinctive advantages in predicting the Rate of Penetration (ROP) during tunnel excavation. The DFF model, with its structured architecture and multiple hidden layers, has demonstrated high accuracy in scenarios where geological conditions are consistent, such as massive rock formations. This precision underscores DFF's strength in leveraging well-defined patterns in static data inputs.

Conversely, the LSTM model excels in dynamic environments characterized by fluctuating geological conditions and variable input parameters. Its ability to incorporate historical data through its recurrent neural network design enables it to adapt and predict future outcomes effectively, making it particularly valuable for environments like highly fractured granite, where geological variables are less predictable.

A crucial insight from this study is the comparative analysis of model performance across different geological contexts. It was observed that both models show enhanced performance in massive rock compared to highly fractured granite. This differentiation highlights the models' capability to identify and learn from complex patterns within more uniform geological structures, which allows for more accurate predictions in these settings. Furthermore, when comparing our integrated approach of using block models combined with deep learning techniques to traditional theoretical and empirical models, our method offers substantial improvements. The integration enhances the adaptability and accuracy of predictions, especially in complex geological conditions that traditional models struggle to interpret effectively. For example, while the CSM and Yagiz models provided foundational insights, our approach reduces RMSE significantly, indicating more precise and reliable predictions.

Ultimately, the findings from this research lay the groundwork for the future development of an advanced ROP prediction framework specifically designed for diverse tunneling scenarios. By harnessing the strengths of both DFF's precision and LSTM's flexibility, this proposed framework promises to revolutionize tunnel excavation planning and execution. It offers the potential not only to improve project efficiency and cost-effectiveness but also to enhance safety and risk management by providing more accurate and timely predictive insights.

This study's implications extend beyond immediate project applications, suggesting broader utility in geotechnical engineering and construction management. The integration of such deep learning models into standard practice could provide substantial benefits, from strategic project planning to real-time decision support, marking a significant step forward in the field of tunnel construction.

8. REFERENCES

AACE. (2005). "TCM Framework:7.3 - Cost Estimating and Budgeting." In: *Cost Estimate Classification System - As Applied in Engineering, Procurement, and Construction for the Process Industries.*

Armaghani, D. J. et al. (2018). "Performance Prediction of Tunnel Boring Machine through Development a Gene Expression Programming Equation." *Engineering with Computers,* Issue 34, 129-141.

Bruland, A. (2000a). "Performance Data and Back-Mapping." In: *Hard Rock Tunnel Boring,* Vol. 6, Trondheim, Norway: Norwegian University of Science and Technology, Department of Building and Construction Engineering.

Bruland, A. (2000b). "The Boring Process." In: *Hard Rock Tunnel Boring,* Vol. 7, Trondheim, Norway: Norwegian University of Science and Technology, Department of Building and Construction Engineering.

Farrokh, E. (2012). "Study of Utilization Factor and Advance Rate of Hard Rock TBMs." *PhD Thesis Dissertation, Department of Energy and Minerals Engineering, The Pennsylvania State University.*

Farrokh, E. et al. (2012). "Study of Various Models for Estimation of Penetration Rate of Hard Rock TBMs." *Tunnelling and Underground Space Technology Incorporating Trenchless Research,* Issue 30, 110-123.

Fattahi, H. and Babanouri, N. (2017). "Applying Optimized Support Vector Regression Models for Prediction of Tunnel Boring Machine Performance." *Geotech. Geol. Eng.,* Issue 35, 2205-2217.

Ghaemi, M. et al. (2015). "Analyzing Schmidt Hammer in Evaluating Compressive Strength of Rock Mass." *EUROCK 2015 & 64th Geomechanics Colloquium.*

Gerhing, K. (1995). "Leistungs- und Verschleiβprognose im maschinellen Tunnelbau." *Felsbau Magazin,* Issue 13.

Hochreiter, S., and Schmidhuber, J. (1997). "Long Short-Term Memory." *Neural Computation,* 9(8), 735-1780.

Kaewkongkaew, K. et al. (2013). "Geological Model of Mae Tang-Mae Ngad Diversion Tunnel Project, Northern Thailand." *Open Journal of Geology,* Issue 3, 340-351.

Koopialipoor, M. et al. (2019). "Predicting Tunnel Boring Machine Performance through a New Model Based on the Group Method of Data Handling." *Bulletin of Engineering Geology and the Environment,* Issue 78, 3799-3813.

Koopialipoor, M. et al. (2020). "Development of a New Hybrid ANN for Solving a Geotechnical Problem Related to Tunnel Boring Machine Performance." *Engineering with Computers,* Issue 36, 345-357.

Macias, F. (2016). "Hard Rock Tunnel Boring: Performance Predictions and Cutter Life Assessment." *PhD Thesis, Norwegian University of Science and Technology, Faculty of Engineering Science and Technology, Department of Civil and Transport Engineering.*

Poniewierski, J. (2019). "Block Model Knowledge for Mining Engineers - An Introduction." ACADEMIA.

Pandey, P.K. et al. (2020). "Influence of Geology on Tunnel Boring Machine Performance - A Review." *Journal of Mining and Metallurgy,* 1-14.

Paraskevopoulou, C., and Boutsis, G. (2020). "Cost Overruns in Tunnelling Projects : Investigating the Impact of Geological and Geotechnical Uncertainty Using Case Studies." *Infrastructures.*

Rostami, J. (1997). "Development of a Force Estimation Model for Rock Fragmentation with Disc Cutters through Theoretical Modeling and Physical Measurement of Crushed Zone Pressure." *PhD Thesis Dissertation, Colorado School of Mines, Golden, Colorado, USA.*

Rostami, J. (2016). "Performance Prediction of Hard Rock Tunnel Boring Machine (TBMs) in Difficult Ground." *Tunnelling and Underground Space Technology,* Issue 57, 173-182.

Shangxin, F. et al. (2021). "Tunnel Boring Machine Performance Prediction: A Case Study Using Big Data and Deep Learning." *Tunnelling and Underground Space Tecnology Incorporating Trenchless Technology Research,* 110.

Sirinart, T. (2017). *Long Short-Term Memory (LSTM).* [Online] Available at: https://medium.com/@sinart.t/long-short-term-memory-lstm-e6cb23b494c6 [Accessed April 2022].

Wilfing, L. (2016). "The Influence of Geotechnical Parameters on Penetration Prediction in TBM Tunnelling in Hard Rock." *PhD, Technische Universität München.*

Yagiz, S. (2002). "Development of Rock Fracture and Brittleness Indiced to Qualify the Effects of Rock Mass Fracture and Toughness in the CSM Model Basic Penetration for Hard Rock Tunnelling Machines." *Thesis, Colorado School of Mines, Golden, Colorado, USA.*

Yagiz, S. (2006). "TBM Performance Prediction Based on Rock Properties." *EUROCK.*